

Electronic Supplementary Information

Conformational and spectroscopic properties of π -extended, bipyrrole-fused rubyrin and sapphyrin derivatives

Se-Young Kee,[†] Jong Min Lim,[¶] Soo-Jin Kim,[†] Jaeduk Yoo,[†] Jung-Su Park,[‡] Tridib Sarma,[€] Vincent M. Lynch,[‡] Pradeeptha K. Panda,^{*,€} Jonathan L. Sessler^{*,‡,¶}, Dongho Kim,^{*,¶} and Chang-Hee Lee^{*,†}

[†]Department of Chemistry and Institute of Molecular Science and Fusion Technology, Kangwon National University, Chun-Chon 200-701, Korea, [‡]Department of Chemistry and Biochemistry University of Texas at Austin, Austin TX 78712 USA, [¶]Department of Chemistry, Yonsei University, Seoul 120-749, Korea, [€]School of Chemistry, University of Hyderabad Hyderabad-500046, India

sessler@mail.utexas.edu; dongho@yonsei.ac.kr; chhlee@kangwon.ac.kr; pkpsc@uohyd.ernet.in

Synthetic procedures; optical and X-ray experimental	-----	S1
Figure S1. ^1H NMR spectrum of naphthorubyrin [2•HCl] in DMSO- d_6	-----	S5
Figure S2. ^1H NMR spectra of naphthorubyrin [2•HCl] in CDCl ₃ , DMSO- d_6	-----	S5
Figure S3. ^{13}C NMR spectrum of naphthorubyrin [2•HCl] in CDCl ₃	-----	S6
Figure S4. MALDI-TOF Mass spectrum of naphthorubyrin [2•HCl]	-----	S7
Figure S5. ^1H NMR spectrum of naphthosapphyrin (3) in CDCl ₃	-----	S8
Figure S6. ^{13}C NMR spectrum of naphthosapphyrin (3) in CDCl ₃	-----	S8
Figure S7. MALDI-TOF Mass spectrum of naphthosapphyrin (3)	-----	S9
Figure S8. ^1H NMR spectral changes of naphthorubyrin (2) in DMSO- d_6 upon addition of TEA	-----	S10
Figure S9. ^1H NMR spectral changes of naphthorubyrin (2) in DMSO- d_6 upon addition of TFA	-----	S10
Figure S10. ^1H NMR spectra of the protonated forms of naphthorubyrin (2) in DMSO- d_6	-----	S11
Figure S11. ^1H NMR spectral changes of naphthosapphyrin (3) in CDCl ₃ seen upon addition of TFA	-----	S12
Figure S12. UV-vis spectra of naphthorubyrin (2) and its mono-protonated and deprotonated forms in CH ₂ Cl ₂ .	---	S13
Figure S13. UV-vis spectral changes of naphthosapphyrin (3) in CH ₂ Cl ₂ seen upon addition of TFA	-----	S14
Figure S14. Comparison of UV-vis absorption spectra of naphthosapphyrin (3) recorded in the absence and in the presence of increasing quantities of trifluoroacetic acid in CH ₂ Cl ₂	-----	S14
Figure S15. ORTEP drawings of the single crystal X-ray structure of naphthorubyrin [2•HCl].	-----	S15
Figure S16. Femtosecond transient absorption spectra and decay profiles of naphthorubyrin (2)	-----	S16
Figure S17. Femtosecond transient absorption spectra and decay profiles of naphthosapphyrin (3)	-----	S17
Figure S18. Decay-associated spectra of neutral naphthosapphyrin (3) and monoprotonated naphthosapphyrin ([3•H] ⁺)	-----	
		S18
References	-----	S19

Synthetic Experimental Section

¹H NMR spectra (300 MHz, Bruker AvanceTM and 400 MHz, Bruker AvanceTM) were recorded using TMS as the internal standard. High resolution mass spectra were obtained on an Voyager-DE STR MALDI-TOF mass spectrometer. Column chromatography was performed over silica gel (Merck, 230-400 mesh). All other reagents were obtained from Aldrich and used as received unless noted otherwise. Naphthobipyrrole **1** was prepared by subjecting the corresponding diethyl ester^[1] to saponification and decarboxylation as follows: A mixture of diethyl 1,10-dihydro-benzo[e]pyrrolo[3,2-g]indole-2,9-dicarboxylate (1 g, 2.85 mmol) and potassium hydroxide (1.26 g, 10 equiv.) was heated at reflux in ethylene glycol (30 mL) under an nitrogen atmosphere for 3 hrs. The reaction was then cooled to room temperature and diluted with cold water (50 mL). The resulting precipitate was collected by filtration and redissolved in dichloromethane. The resulting solution was dried over anhydrous Na₂SO₄ and then filtered. The volatiles were removed in *vacuo*. Yield 0.46 g (78%); ¹H NMR (300 MHz, DMSO-*d*₆) δ 11.0 (br s, 2H), 8.21-8.15 (m, 2H), 7.38-7.32 (m, 2H), 7.24 (t, *J* = 2.67 Hz, 2H), 7.03-7.01 (m, 2H).

Naphthorubyrin (**2•HCl**) and Naphthosapphirin (**3**)

Naphthobipyrrole (0.10 g, 0.49 mmol), pyrrole (0.034 mL, 0.49 mmol), pentafluorobenzaldehyde (0.12 mL, 0.97 mmol) were dissolved in CH₂Cl₂ (180 mL) and then TFA (0.037 mL, 0.49 mmol) was added. The mixture was stirred for 7 days at room temperature. At this point, DDQ (0.33 g, 1.46 mmol) was added and the reaction was stirred at room temperature for an additional 1 hr. The reaction was quenched by adding TEA (0.27 mL, 1.94 mmol). The reaction mixture was then washed with water (50 mL) and extracted with CH₂Cl₂. The organic layer was dried (Na₂SO₄) and the volatiles were removed in *vacuo*. In order to separate the desired fraction, a first column chromatographic separation was performed as follow: The fast moving red fraction observed on a silica gel column upon eluting with CHCl₃ was collected first. The eluent was then changed to CHCl₃/hexanes (8/2) and the slow moving purple fraction was collected. As inferred from a preliminary mass spectrometric analysis, the red fraction contained mostly (**3**). This product was then purified by subjecting it to a second column chromatographic purification over silica gel (eluent: CHCl₃/hexanes = 8/2). The purple fraction was likewise considered to contain mostly (**2•HCl**) and was purified by subjecting it to a second round of column chromatography over silica gel (eluent: CHCl₃). Yield for (**2•HCl**) 0.012 g (2%); UV-vis. (CH₂Cl₂) λ_{max} (log ε) 528 nm (5.17), 582 nm (5.05), 868 nm (4.83); ¹H NMR (300 MHz, DMSO-*d*₆) δ 11.13 (s, 2H), 10.98 (s, 2H), 9.70-9.67 (m, 2H), 9.64 (s, 2H), 9.62-9.59 (m, 2H), 9.43 (s, 2H), 8.15-8.12 (m, 4H), -1.96 (br s, 2H), -2.60 (br s, 2H), -2.69(br s, 1H); ¹³C NMR (400 MHz, CDCl₃) δ 153.5, 148.5, 148.1, 146.83, 146.5, 141.9, 139.1, 138.9, 137.6, 137.3, 135.4, 133.0, 132.5, 131.7, 131.6, 129.4, 129.3, 128.2, 127.6, 127.4, 123.3, 122.2, 119.4, 118.9, 118.7, 117.7, 105.1, 94.3; MALDI-TOF MS Calcd. for C₆₄H₂₁F₂₀N₆⁺ 1253.8593, Found 1253.2770 (M + H⁺). Yield for (**3**) ; 0.011 g (2%); UV-vis. (CH₂Cl₂) λ_{max} (log ε) 502 nm (5.32), 527 nm (5.23), 711 nm (4.34), ; ¹H NMR (300 MHz, CDCl₃) δ 11.00 (br s, 1H), 9.53 (s, 2H), 9.00-8.98

(m, 2H), 8.74-8.70 (m, 4H), 7.87-7.84 (m, 2H), -0.33(br s, 2H), -0.73 (s, 2H); ^{13}C NMR (400 MHz, CDCl_3) δ 156.4, 150.5, 145.0, 136.5, 133.7, 132.8, 129.6, 129.1, 128.2, 128.0, 125.8, 125.2, 117.6, 114.7, 112.5, 107.2, 100.9; MALDI-TOF MS Calcd. for $\text{C}_{54}\text{H}_{15}\text{F}_{20}\text{N}_5$ 1113.6985, Found 1114.2290 ($\text{M} + \text{H}^+$).

Time-resolved Optical Studies

Femtosecond time-resolved transient absorption (TA) spectra were recorded using a spectrometer consisting of a homemade noncollinear optical parametric amplifier (NOPA) pumped by a Ti:sapphire regenerative amplifier system (Quantronix, Integra-C) operating at 1 kHz repetition rate coupled with an optical detection system. The generated visible NOPA pulses had a pulse width of \sim 100 fs and an average power of 1 mW in the range 480-700 nm, which were used as pump pulses. White light continuum (WLC) probe pulses were generated using a sapphire window (2 mm of thickness) by focusing of small portion of the fundamental 800 nm pulses that were picked off by a quartz plate before entering to the NOPA. The time delay between pump and probe beams was carefully controlled by causing the pump beam to travel along a variable optical delay (Newport, ILS250). The intensities of the spectrally dispersed WLC probe pulses were monitored by means of a miniature spectrograph (OceanOptics, USB2000+). To obtain the time-resolved transient absorption difference signal (ΔA) at a specific time, the pump pulses were chopped at 25 Hz and the absorption spectra intensities were saved alternately with or without pump pulse. Typically, 6000 pulses were used to excite the samples so as to obtain a TA spectra at a particular delay time. The polarization angle between the pump and probe beams was set at the magic angle (54.7°) using a Glan-laser polarizer with a half-wave retarder so as to prevent polarization-dependent signals. The cross-correlation fwhm in the pump-probe experiments was less than 200 fs and the chirp of WLC probe pulses was measured to be 800 fs in the 400-800 nm region. To minimize chirp, all-reflection optics in the probe beam path and a 2 mm path length quartz cell were used. After completing the fluorescence and TA experiments, the absorption spectra of all compounds was carefully checked so as to avoid artifacts arising from, e.g., photo-degradation or photo-oxidation of the samples in question. HPLC grade solvents were used in all steady-state and time-resolved spectroscopic studies. Decay associated spectra were calculated by using an external software program (Surface Explorer Pro, Ultrafast Systems) with chirp compensation and the singular value deposition method retrieved from the time-resolved TA spectra. To observe the steady-state fluorescence spectra in the NIR region, a photomultiplier tube (Hamamatsu, R5108), a lock-in amplifier (EG&G, 5210) combined with a mechanical chopper, and a Ti:Sapphire laser (Coherent, Verdi) for photo-excitation at 532 nm were used.

Crystallographic analysis of **2•HCl**:

Crystals were grown as black needles by slow diffusion of hexane into chloroform solution of **2**. The data crystal was cut from a cluster of crystals and had approximate dimensions; 0.25 x 0.07 x 0.05 mm. X-ray crystallographic data for **2•HCl** were collected at -50 °C on a Rigaku SCX-Mini diffractometer using a monochromatized MoK_a source ($\lambda = 0.71075 \text{ \AA}$) equipped with a Mercury CCD area detector. A total of 431 frames of data were collected using ω -scans with a scan range of 1° and a counting time of 70 seconds per frame. The frame data were integrated and corrected for absorption effects using the Rigaku/MSC CrystalClear program package.^[2]

The structure was solved by direct methods and refined by full-matrix least-squares on F² with anisotropic displacement parameters for the non-H atoms using SHELXL-97.^[3] The function, $\Sigma w(|Fo|^2 - |Fc|^2)^2$, was minimized, where $w = 1/[(|Fo|)^2 + (X^*P)^2 + (Y^*P)]$ and $P = (|Fo|^2 + 2|Fc|^2)/3$ and the parameters, X and Y, are suggested during the refinement process. The hydrogen atoms were calculated in ideal positions with isotropic displacement parameters set to 1.2xUeq of the attached atom (1.5xUeq for methyl hydrogen atoms). Neutral atom scattering factors and values used to calculate the linear absorption coefficient are from the International Tables for X-ray Crystallography (1992).^[4] Further details of the refinement and structure are listed in Table S1 below and can be obtained from the Cambridge Crystallographic Data Centre by quoting CCDC 812383.

Table S1. Crystal data and structure refinement for Naphtharubyrin, **2•2HCl.**

Empirical formula	C76 H48 Cl5 F20 N6
Formula weight	1602.45
Temperature	233(2) K
Wavelength	0.71075 Å
Crystal system, space group	Tetragonal, $\bar{4} 2_1/m$
Unit cell dimensions	$a = 21.411(2) \text{ \AA}$ alpha = 90 deg.; $b = 21.411(2) \text{ \AA}$ beta =
90 deg.; $c = 7.5217(8) \text{ \AA}$	gamma = 90 deg.
Volume	3448.2(7) \AA^3
Z, Calculated density	2, 1.543 Mg/m ³
Absorption coefficient	0.316 mm ⁻¹
F(000)	1622
Crystal size	0.25 x 0.07 x 0.05 mm
Theta range for data collection	3.01 to 25.00 deg.
Limiting indices	-24 <= h <= 25, -25 <= k <= 25, -8 <= l <= 8
Reflections collected / unique	19139 / 1742 [R(int) = 0.0938]
Completeness to theta =	25.00 97.4 %
Absorption correction	Semi-empirical from equivalents
Max. and min. transmission	1.00 and 0.782
Refinement method	Full-matrix least-squares on F ²
Data / restraints / parameters	1742 / 81 / 281
Goodness-of-fit on F ²	1.182
Final R indices [I>2sigma(I)]	R ₁ = 0.0526, wR ₂ = 0.1248
R indices (all data)	R ₁ = 0.0877, wR ₂ = 0.1409
Largest diff. peak and hole	0.318 and -0.225 e.A ⁻³

Figure S1. ^1H NMR spectrum of naphthorubyrin (**2•HCl**) in $\text{DMSO}-d_6$.

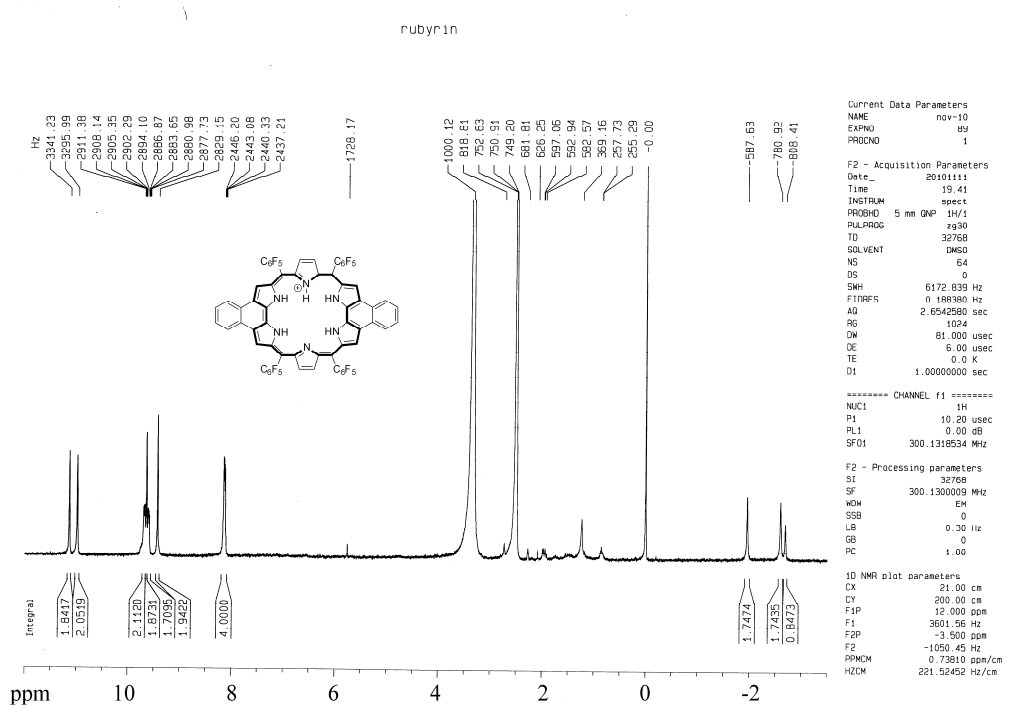


Figure S2. ^1H NMR spectra of naphthorubyrin (**2•HCl**) in CDCl_3 and $\text{DMSO}-d_6$.

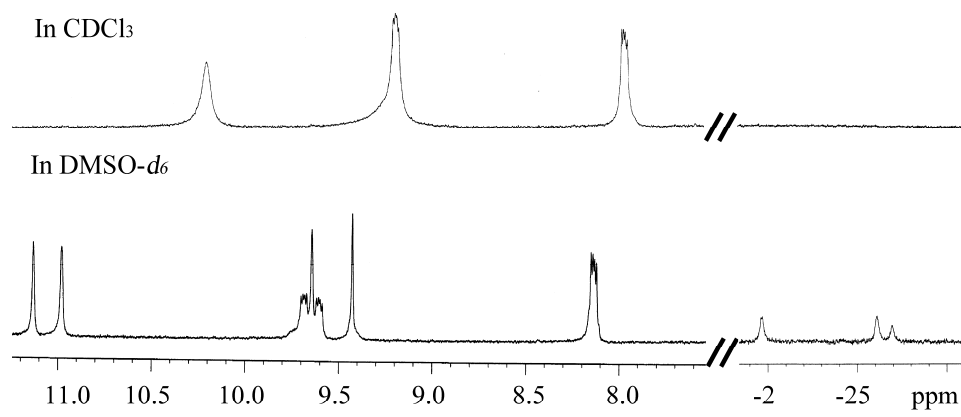


Figure S3. ^{13}C NMR spectrum of naphthorubyrin (**2**•HCl) in $\text{DMSO}-d_6$.

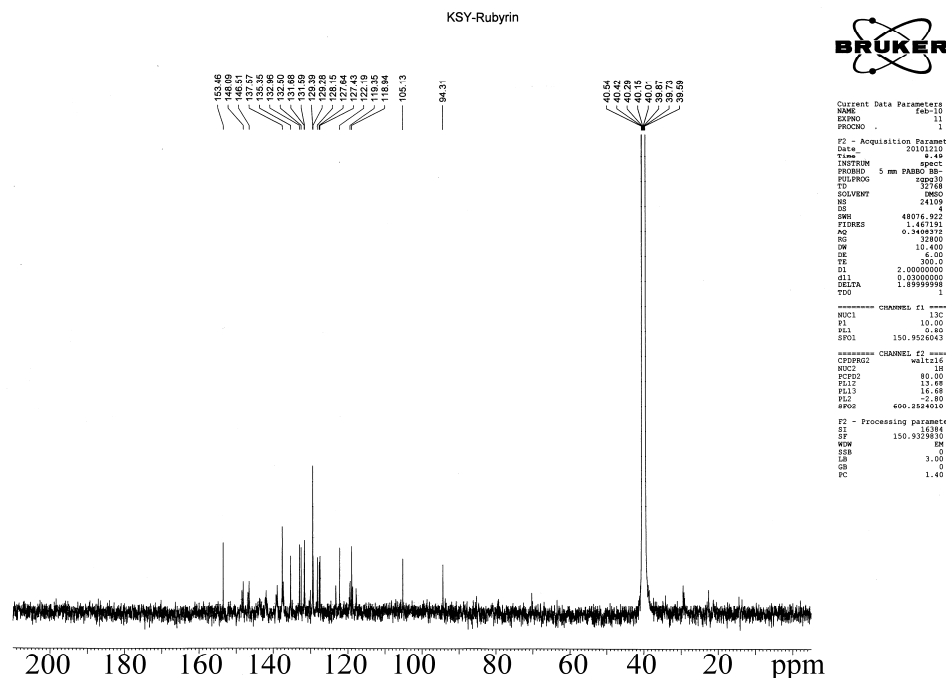


Figure S4. MALDI-TOF Mass spectrum of naphthorubyrin ($[2\bullet H]^+$).

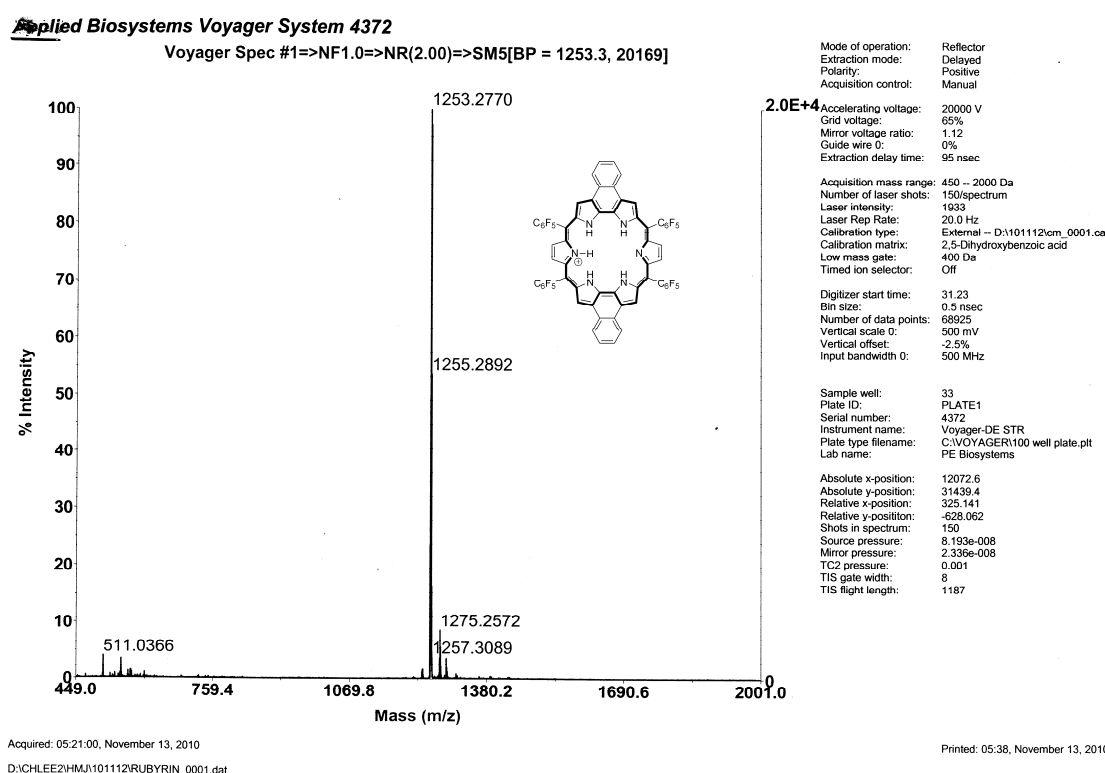


Figure S5. ^1H NMR spectrum of naphthosapphyrin (**3**) recorded in CDCl_3 .

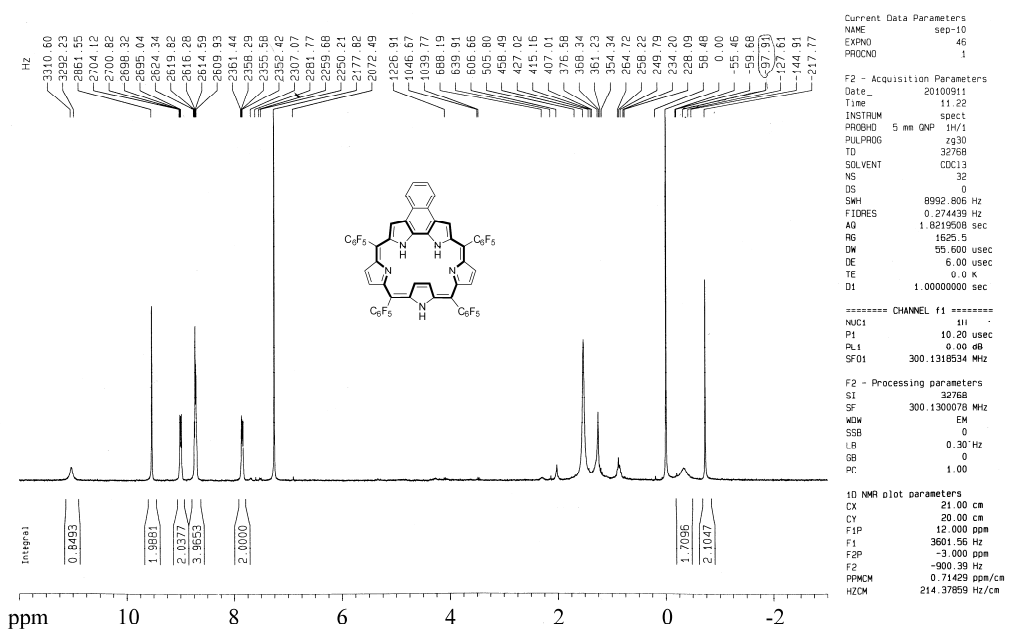


Figure S6. ^{13}C NMR spectrum of naphthosapphyrin (**3**) recorded in CDCl_3 .

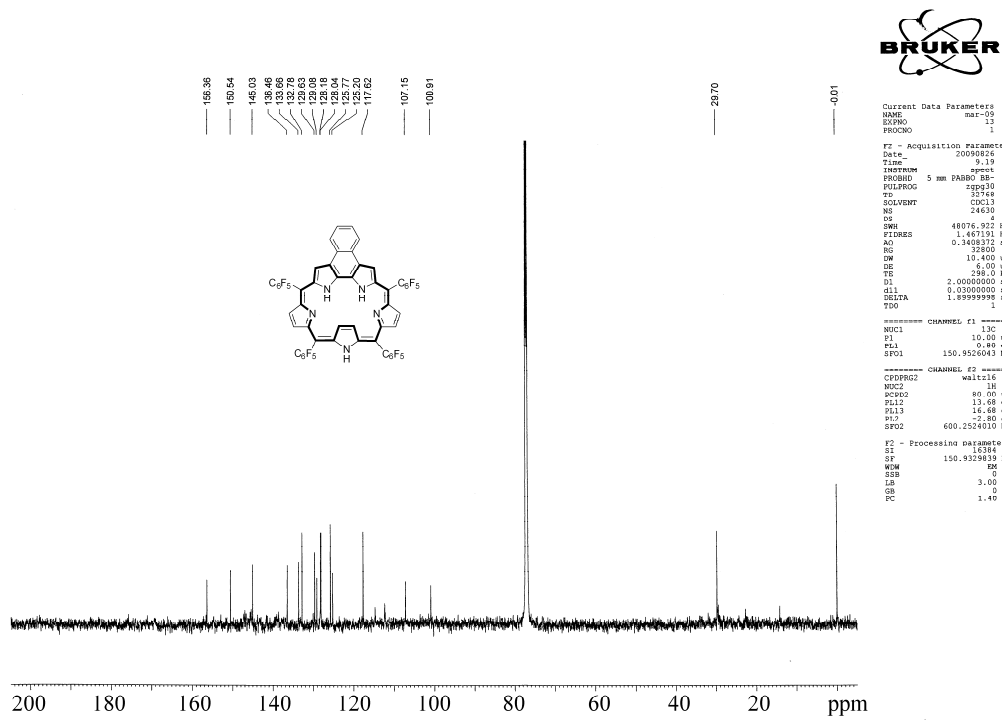


Figure S7. MALDI-TOF Mass spectrum of naphthosapphyrin (**3**)

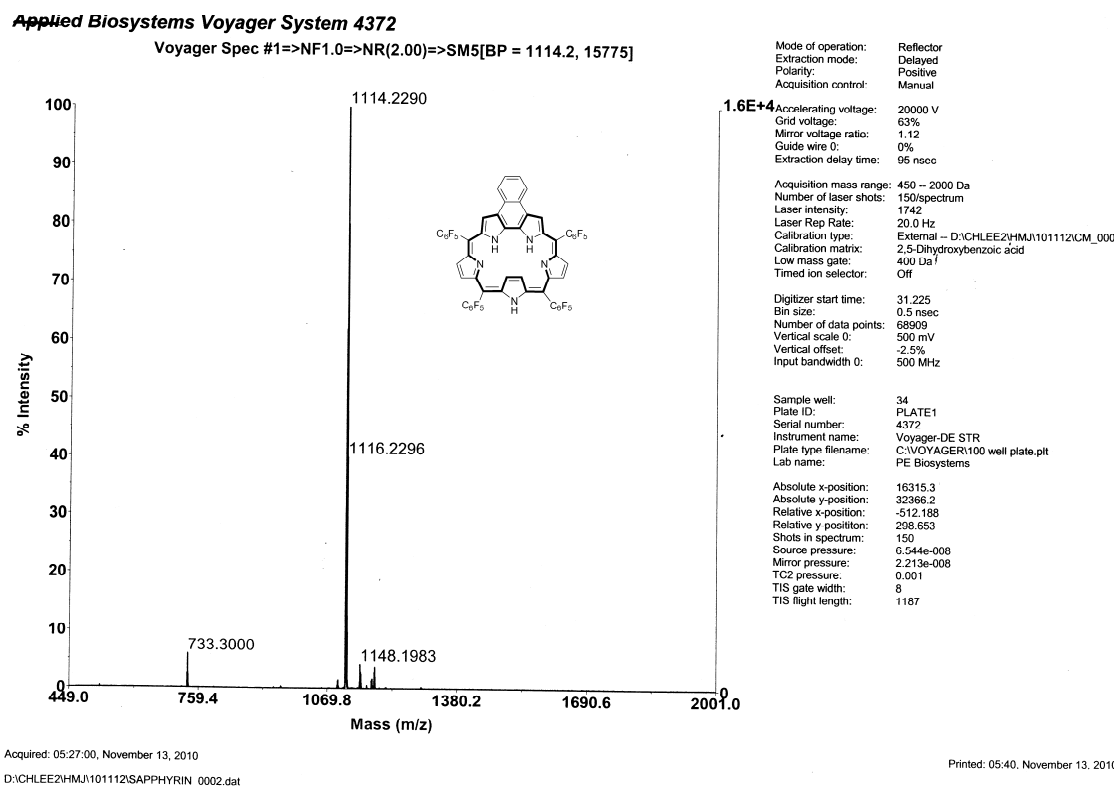


Figure S8. ^1H NMR spectral changes for mono-protonated naphthorubyrin (**2**• HCl) (6.38×10^{-4} M in $\text{DMSO}-d_6$) seen upon the addition of triethylamine (TEA).

Mono - protonated (**2**• H^+Cl^-)

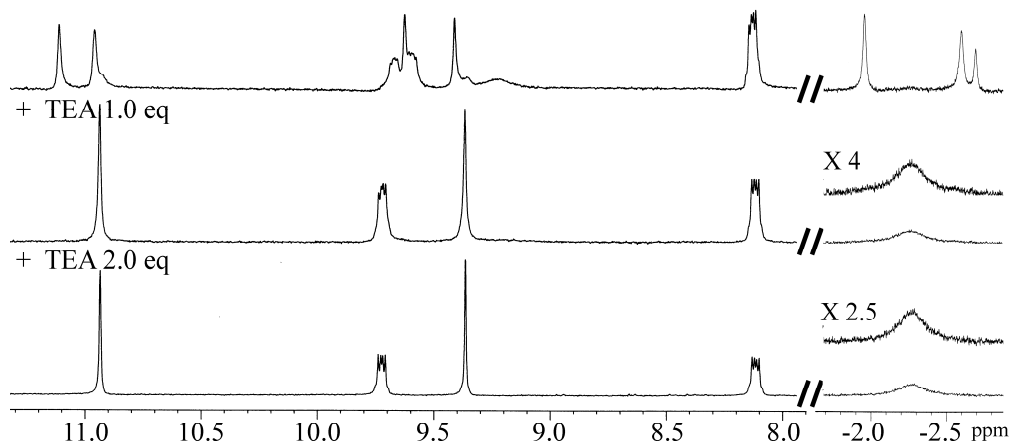


Figure S9. ^1H NMR spectral changes for mono-protonated naphthorubyrin (**2**• HCl) (1.60×10^{-3} M in $\text{DMSO}-d_6$) seen upon the addition of trifluoroacetic acid (TFA).

Mono - protonated (**2**• H^+Cl^-)

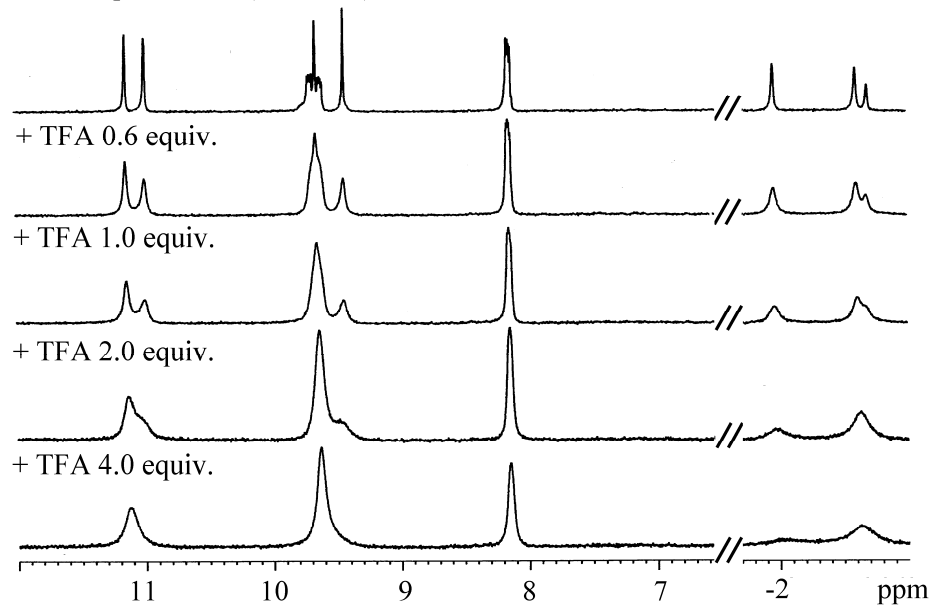
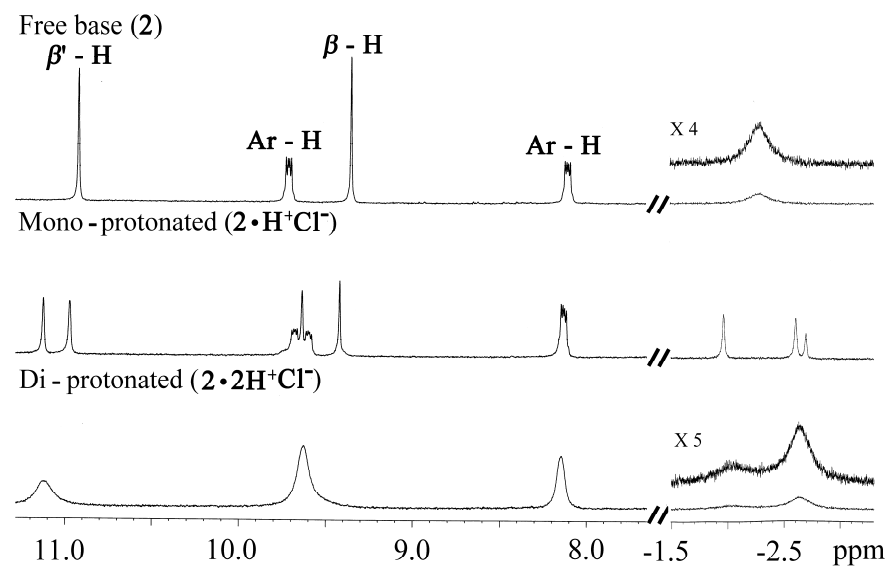


Figure S10. ^1H NMR spectra of naphthorubyrin (**2**) and its mono-protonated ($[\mathbf{2}\bullet\text{H}]^+$) and di-protonated ($[\mathbf{2}\bullet\mathbf{2}\text{H}]^{2+}$) forms recorded in $\text{DMSO}-d_6$. Here, naphthorubyrin **2** was treated initially with one equiv, followed by a large excess (ca. 200 equiv.), of TFA in $\text{DMSO}-d_6$; $[\mathbf{2}] = 5.32 \text{ mM}$.



Note that salt $[\mathbf{2}\bullet\text{HCl}]$ displays three distinctive NH resonances at -2.67 (2H), -2.61 (2H) and -1.97 (1H) ppm in the proton NMR spectrum. Treatment of $[\mathbf{2}\bullet\text{HCl}]$ with a molar excess of triethylamine (ca. 2 equiv) results in complete deprotonation and affords the free-base form, which displays an NH signal integrating to four protons, that are inferred to lie within the core. When free-base rubyrin **2** is treated with 1 equiv of trifluoroacetic acid, reprotonation occurs to produce $[\mathbf{2}\bullet\text{H}]^+$. This results in a loss in symmetry as inferred from the above ^1H NMR spectroscopic analyses.

Figure S11. ^1H NMR spectral changes for naphthosapphyrin (**3**) (7.18×10^{-3} M in CDCl_3) seen upon the addition of TFA.

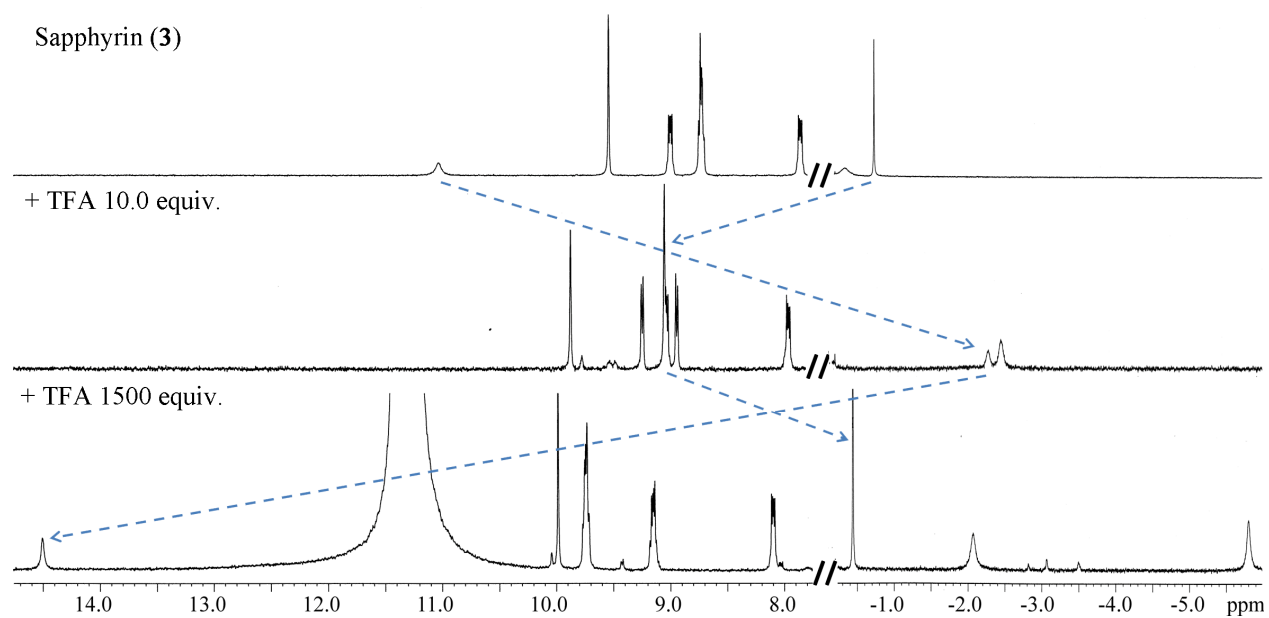


Figure S12. Comparison of the UV/Vis absorption spectra for the mono- and di-protonated forms of naphthorubyrin **2**. The spectra were recorded by treating the free-base form of **2** ($[2] = 8.33 \mu\text{M}$ in CH_2Cl_2). Treatment with 1 equiv of TFA gave the mono-protonated form, and ca. 200 equiv of TFA was then added to ensure near-complete conversion to the diprotonated form. The blue lines are the corresponding fluorescence emission spectra.

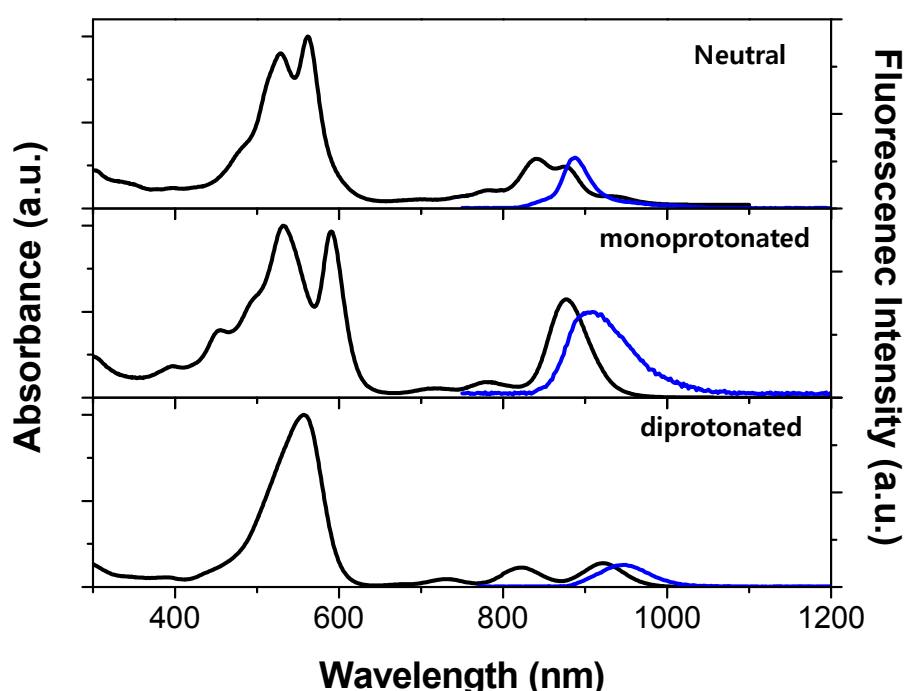


Figure S13. UV-vis absorption spectral changes for naphthosapphyrin (**3**) (8.33×10^{-6} M in CH_2Cl_2) seen upon the addition of TFA.

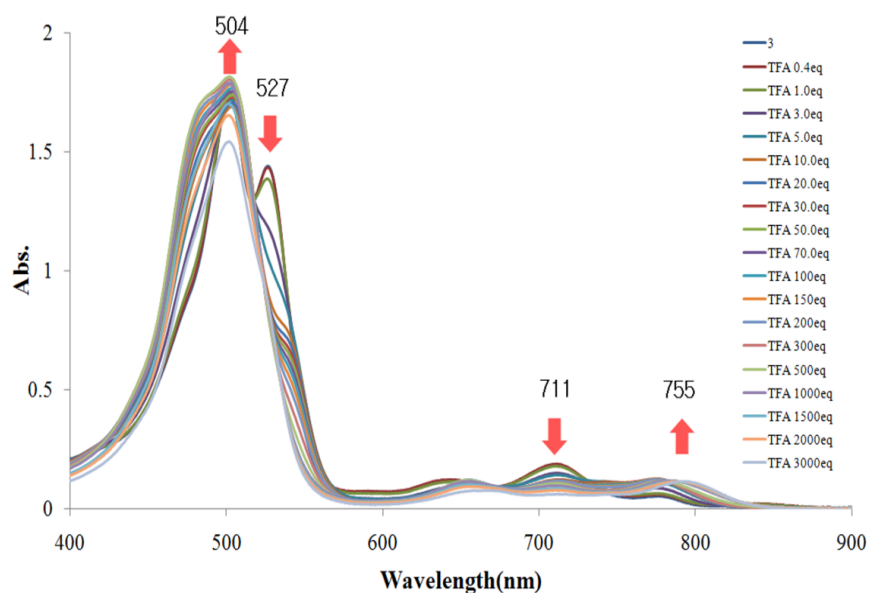


Figure S14. Comparison of UV-vis absorption spectra of naphthosapphyrin **3** recorded in the absence and presence of increasing quantities of trifluoroacetic acid in CH_2Cl_2 ($[3] = 8.46 \times 10^{-6}$ M). The spectra labeled as “Neutral”, “monoprotonated” and “diprotonated” were measured in the presence of 0, 10, and 1500 equiv of acid, respectively. The blue traces show the corresponding emission spectra.

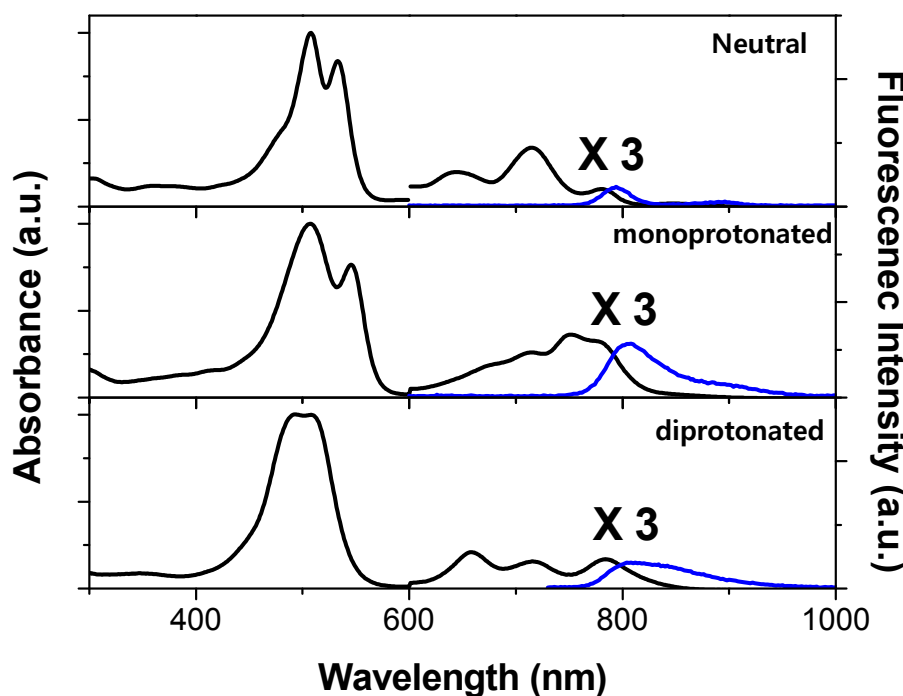


Figure S15. ORTEP drawings of the single crystal X-ray structure of naphthorubyrin [2•HCl].

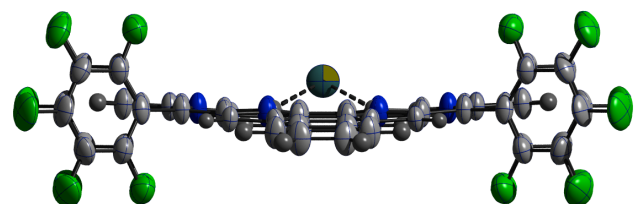
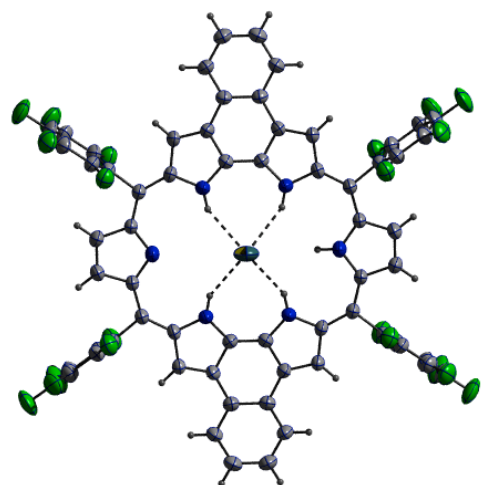


Figure S16. Femtosecond transient absorption spectra and decay profiles of naphthorubyrin **2** (a) and its protonated (b; monoprotonated, c; deprotonated) forms recorded in toluene.

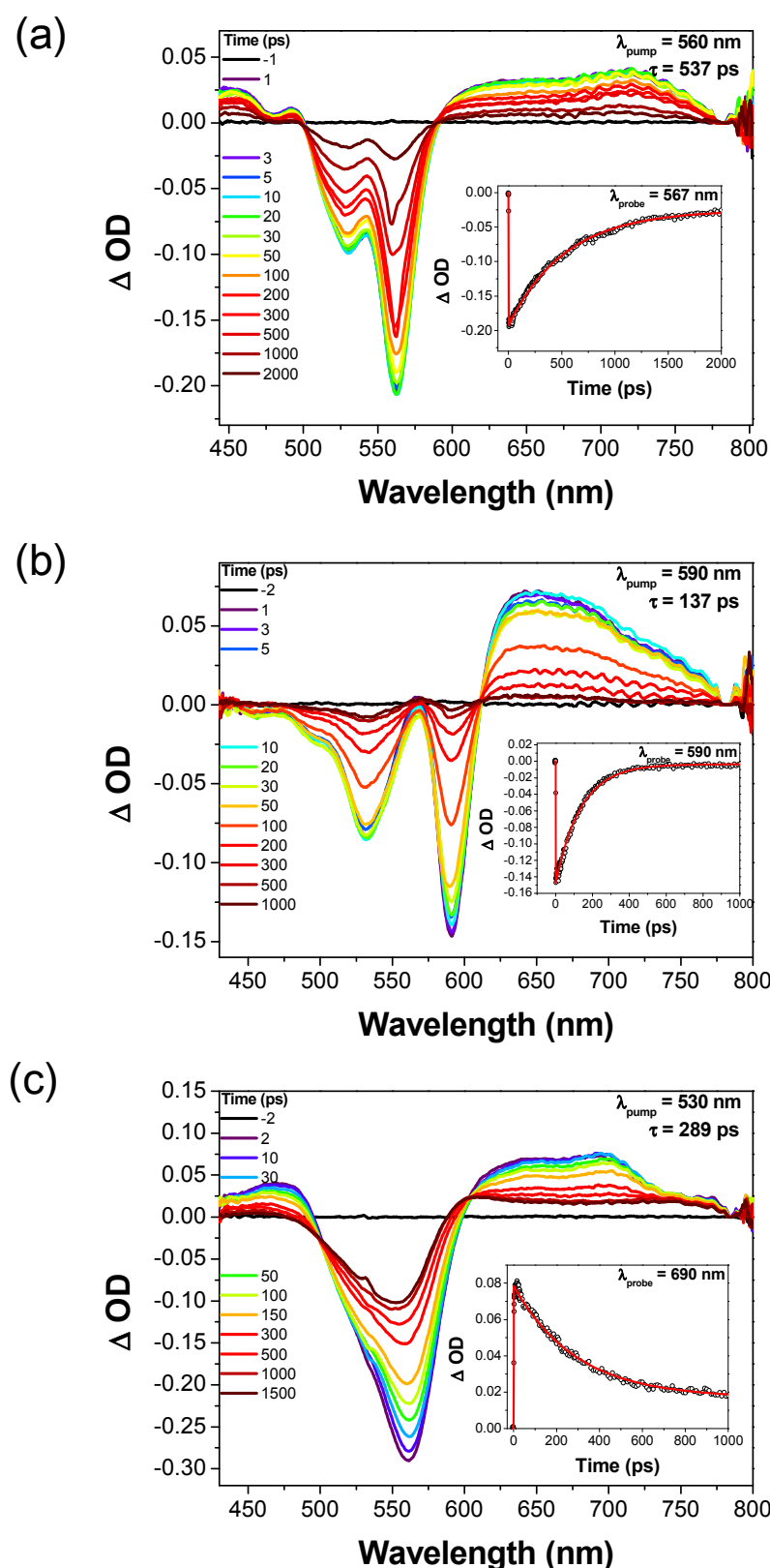


Figure S17. Femtosecond transient absorption spectra and decay profiles of naphthosapphyrin **3** (a) and its protonated (b; monoprotonated, c; deprotonated) forms in toluene.

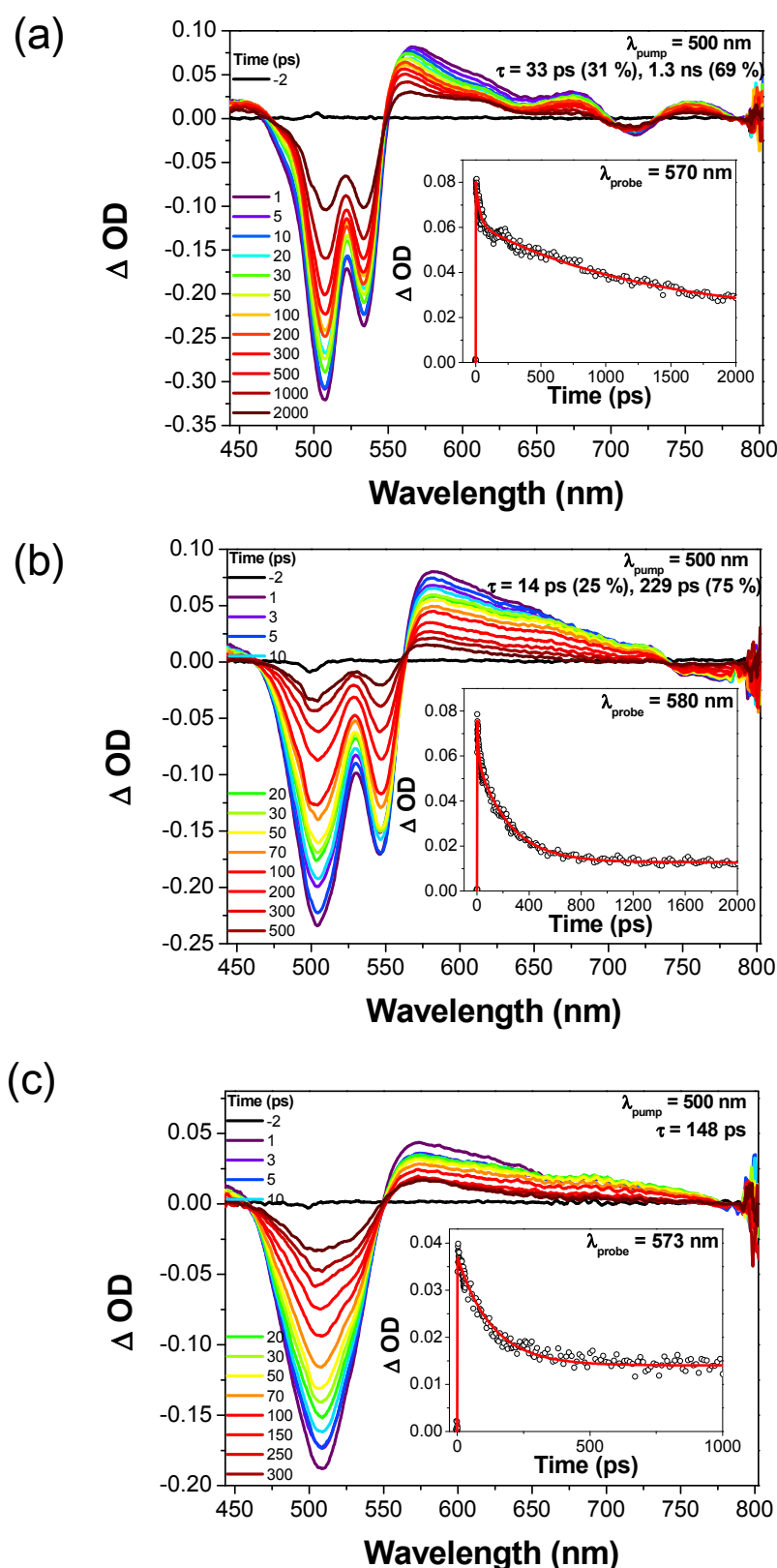
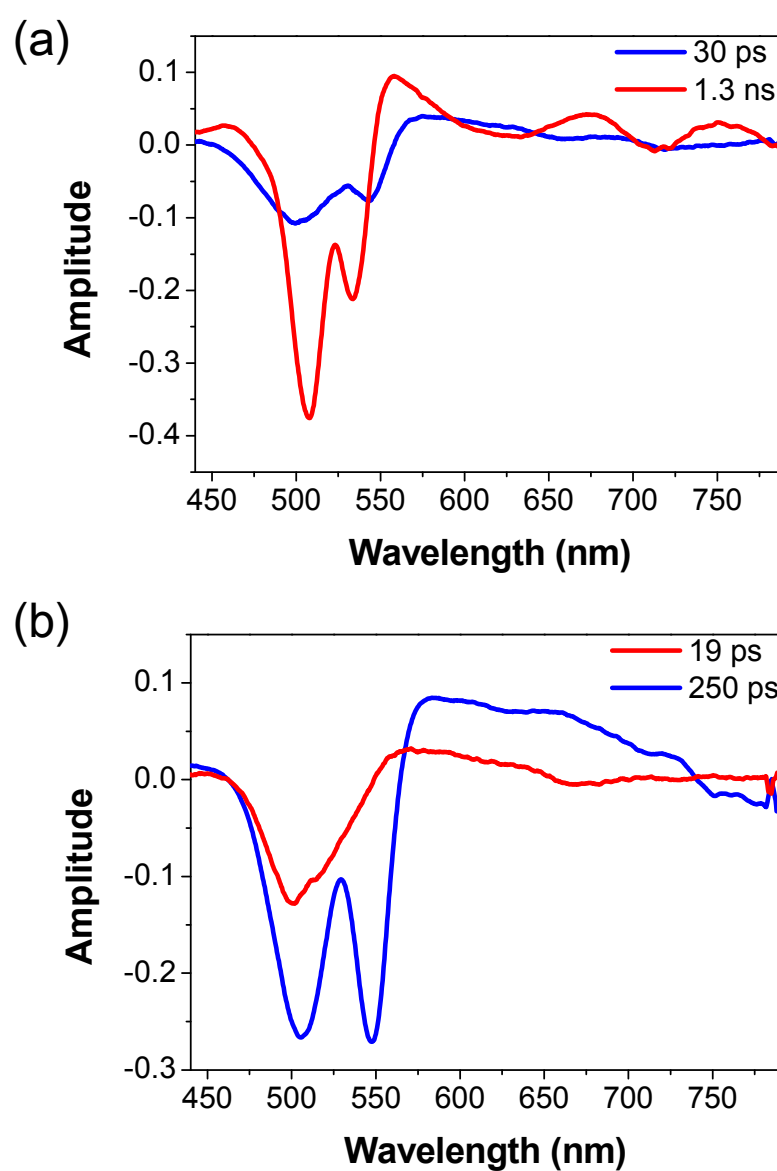


Figure S18. Decay-associated spectra of neutral naphthosapphyrin (**3**; a) and monoprotonated naphthosapphyrin ($[3 \cdot H]^+$; b) from measurements carried out in toluene.



References for ESI

1. R. Roznyatovskiy, V. Lynch, J. L. Sessler, *Org. Lett.* **2010**, *12*, 4424-44270.
2. CrystalClear 1.40 (2008). Rigaku Americas Corporation, The Woodlands, TX.
3. G. M. Sheldrick, SHELXL97. Program for the Refinement of Crystal Structures. University of Gottingen, Germany (**1994**).
4. International Tables for X-ray Crystallography, Vol. C, Tables 4.2.6.8 and 6.1.1.4, A. J. C. Wilson, editor, Boston: Kluwer Academic Press (**1992**).